



Published in final edited form as:

Int J Radiat Oncol Biol Phys. 2015 June 1; 92(2): 407–414. doi:10.1016/j.ijrobp.2015.01.006.

Noninvasive Ultrasonic Nakagami Imaging of Neck Fibrosis following Head-and-Neck Radiotherapy

Xiaofeng Yang, PhD¹, Emi Yoshida, MD², Richard J. Cassidy, MD¹, Jonathan J. Beitler, MD¹, David S. Yu, MD, PhD¹, Walter J. Curran, MD¹, and Tian Liu, PhD¹

¹Department of Radiation Oncology and Winship Cancer Institute, Emory University, Atlanta, GA 30322

²Department of Radiation Oncology, Cedars-Sinai Medical Center, Los Angeles, CA 90048

Abstract

Purpose/Objective(s)—To investigate the feasibility of ultrasound Nakagami imaging to quantitatively assess radiation-induced neck fibrosis – a common sequela of head-and-neck radiotherapy (RT).

Materials and Methods—In a pilot study, 40 subjects were enrolled and classified into 3 subgroups: (1) control group of 12 healthy volunteers, (2) asymptomatic group of 11 patients who have received IMRT for head-and-neck cancer and experienced no neck fibrosis, and (3) symptomatic group of 17 post-RT patients with neck fibrosis. Each subject underwent one ultrasound study in which scans were performed in the longitudinal orientation of the bilateral neck. Three Nakagami parameters were calculated to quantify radiation-induced tissue injury: Nakagami probability distribution function, shape and scaling parameters. Physician-based assessments of the neck fibrosis were performed using RTOG late morbidity scoring scheme, while patient-based fibrosis assessments were rated based on the symptoms such as pain and stiffness.

Results—Major discrepancies existed between physician- and patient-based assessments of radiation-induced fibrosis. Significant differences in all Nakagami parameters were observed between the control group and two post-RT groups. Moreover, significant differences in Nakagami shape and scaling parameters were observed among asymptomatic and symptomatic groups. Compared with the control group, average Nakagami shape parameter value increased by 32.1% ($p < 0.001$) and average Nakagami scaling parameter increased by 55.7% ($p < 0.001$) for the

© 2015 Elsevier Inc. All rights reserved.

Corresponding author: Tian Liu, PhD, Department of Radiation Oncology, Emory University School of Medicine, 1365 Clifton Road NE, Atlanta, GA 30322, Tel: (404)778-1848, Fax: (404)778-4139, tliu34@emory.edu.

This paper has not been published. Part of this paper was presented at the “Best in Physics” session at the 54th Annual Meeting & Exhibition of the American Association of Physicists in Medicine (AAPM) in October 2012.

Conflicts of Interest: None

Publisher's Disclaimer: This is a PDF file of an unedited manuscript that has been accepted for publication. As a service to our customers we are providing this early version of the manuscript. The manuscript will undergo copyediting, typesetting, and review of the resulting proof before it is published in its final citable form. Please note that during the production process errors may be discovered which could affect the content, and all legal disclaimers that apply to the journal pertain.

asymptomatic group, whereas the Nakagami shape parameter increased by 74.1% ($p < 0.001$) and the Nakagami scaling parameter increased by 83.5% ($p < 0.001$) for the symptomatic group.

Conclusions—Ultrasonic Nakagami imaging is a potential, quantitative tool to characterize radiation-induced asymptomatic and symptomatic neck fibrosis.

Introduction

Clinically symptomatic neck fibrosis is a common sequela of radiotherapy (RT) for head-and-neck malignancies (1–4). With a latency period of 1 to 2 years post radiation, fibrosis manifests as a loss of pliability and flexibility of the soft tissue affecting the skin, subcutaneous and underlying soft tissues (2). Associated functional deficits of radiation-induced fibrosis include pain, neuropathy and loss of joint range of motion that negatively affects many patients' quality of life (5–8).

Fibrosis development is characterized by cellular and extracellular architectural changes that can be objectively measured via impractical biopsies or via novel advanced imaging (9). Management of radiation-induced fibrosis is dependent upon identification of fibrosis stage, and on controlled randomized trials to determine treatments effective in targeting each stage (10). In addition, accurate measurement of RT-induced fibrosis becomes crucial as we investigate new strategies that reduce treatment morbidity through variations in fractionation schedule, dosage, delivery method, and chemotherapy regimen (11).

The study's goal is to develop a noninvasive, simple ultrasound imaging tool that can accurately and reliably quantify radiation-induced fibrosis. We propose to use Nakagami-parameter imaging, which is a statistical tool that has been applied in the context of ultrasonic characterization of the biomechanical properties of backscattered radio-frequency (RF) signals from biological tissues. Ultrasound tissue characterization using Nakagami statistics has shown early success in the detection of organ abnormalities, such as breast cancer (12, 13) and liver fibrosis (14). Herein, we report our current efforts in developing a Nakagami parameter imaging tool for radiation-induced neck fibrosis. In what follows, we describe the ultrasound examination of the bilateral neck, summarize the Nakagami statistical model, detail the data processing procedures, and finally demonstrate its potential of providing a quantitative imaging tool to assess radiation-induced fibrosis.

Materials and Methods

Study design and subjects

This cross-sectional ultrasound imaging study of neck fibrosis was approved by the Institutional Review Board. Two groups of subjects were recruited: control group of healthy volunteers and post-RT population who have received RT for their head-and-neck cancers. Since radiation-induced fibrosis has a latency of 1 and 2 years post radiation, we chose to enroll post-RT patients who had completed their head-and-neck RT between 1 and 3 years ago. To address the inhomogeneous dose distribution, we calculated the point doses 1.5 cm deep in the upper, mid and lower neck, both right and left. Areas with low doses ($< 50\text{Gy}$) or inhomogeneous ($> 7\%$ dose variation) distributions were excluded.

The primary outcome was quantification of neck fibrosis using Nakagami ultrasound parameters. The secondary outcome was precision of clinical assessments with respect to patient self-assessments of fibrosis.

Clinical assessment of fibrosis

For all post-RT patients, clinical assessments of fibrosis were performed using both physician's evaluation and patient's questionnaire. First, a radiation oncologist performed a physical examination including visual inspection and palpation of the right and left neck regions. Based on the clinical examination, the physician assigned late toxicity from grade 0 (absent) to grade 3 (severe) using Radiation Therapy Oncology Group (RTOG) late radiation morbidity scoring scheme of subcutaneous-tissue toxicity (15). Next, each patient was asked to rate their right and left neck fibrosis through the level of pain and stiffness in 4 levels: grade 0 (none), grade 1 (mild), grade 2 (moderate), or grade 3 (severe). The physician and the patient were blinded to each other's evaluations.

Ultrasound scanning

Each subject underwent one ultrasound study of the bilateral neck. A standardized protocol for ultrasound scanning was established using a clinical scanner (SonixTouch, Ultrasonix, British Columbia, Canada) with a linear array transducer (L14-5/38 probe, 128 elements). All ultrasound data were acquired with the settings: 10 MHz center frequency, 1.00 cm focal length, 3 cm depth, 72% gain, 31 frames per second, and 80-dB dynamic range. The time-gain-compensation (TGC) was set to the maximum value for all depths. All subjects were scanned in an upright-seated position and bilateral ultrasound scans of the neck were performed in the longitudinal orientation (5 cm across the sternocleidomastoid muscle). Using bony anatomy, the area approximates to the bottom of the transverse process of C2 superiorly to the bottom of the transverse process of C4 or about the top of C5 vertebral body inferiorly. During the ultrasound scan, a thin layer of ultrasound gel was used to ensure sufficient coupling between the neck and the ultrasound probe. The probe was placed perpendicular to the scan surface with minimal pressure applied to the neck.

During the ultrasound examination, B-mode images of the bilateral neck and the corresponding RF echo signals were acquired simultaneously. All B-mode images were saved in 8-bit gray scale, with intensity ranging from 0 to 255. Each B-mode image contained 488 (width) \times 356 (depth) pixels, and the image size was 3.8 cm (width) \times 3.0 cm (depth). In this paper, all B-mode images and corresponding parameter images were displayed to the depth of 2 cm; therefore all image sizes were 3.8 cm (width) \times 2.0 cm (depth). All RF data were acquired at 20 MHz sampling frequency. Each image frame contained 256 scan lines and 784 sample points/line. The Nakagami parameters were generated from the RF signals within a specified region of interest.

Quantitative ultrasound analysis – the Nakagami statistical model

The theoretical framework for Nakagami imaging relates statistical parameters to properties of the examined tissue (16–18). The formulation treats the backscattered ultrasound envelope signals as random signals. Our analysis characterizes tissue structures in terms of a stochastic probability distribution function (PDF) under the Nakagami statistical model. The

PDFs of the ultrasound backscattered envelope X under the Nakagami statistical model is given by:

$$f(x) = \frac{2u^u}{\Gamma(u)\omega^u} x^{2u-1} \exp\left(-\frac{u}{\omega} x^2\right) \cdot W(x) \quad (1)$$

where $\Gamma(\cdot)$ is the gamma function and $W(\cdot)$ is the step function.

The Nakagami distribution has two parameters: scaling and shape. Let $E(\cdot)$ denote the statistical mean. The Nakagami scaling parameter ω is obtained from the following equation:

$$\omega = E(X^2). \quad (2)$$

The Nakagami shape parameter u is estimated from the second and fourth moment of the backscattered envelopes. The Nakagami shape parameter u is obtained from the following equation:

$$u = \frac{E^2[X^2]}{E[X^2 - E(X^2)]^2} \quad (3)$$

When $u = 1$, the Nakagami distribution reduces to a Rayleigh distribution. When $0 < u < 1$, the envelope distribution is considered to be pre-Rayleigh. When $u > 1$, the distribution conforms to post-Rayleigh. This property makes the Nakagami distribution a general model for ultrasound backscattering (19).

We have developed Nakagami statistical analysis procedures to quantitatively characterize neck fibrosis. The procedures were carried out through an in-house MATLAB[®] (Mathworks, Inc., Natick, MA) software routine (Figure 3). The B-mode images are used to identify the overall anatomic structures and guides the region-of interest selection. In an earlier study, we have demonstrated the inter-observer and intra-observer reliability of manual contouring of the parotid glands (20). A 10mm × 35 mm box at 8 mm depth was used as the ROI for the Nakagami statistical analysis. The ultrasound Nakagami parameter images were generated using a square-sliding window to process the envelope image. An inverse relationship exists between the resolution and statistical stability of the Nakagami estimation. In our study, the incident pulse length was approximately 0.3 mm and we used a sliding window size of 1.8×1.8 mm. The scaling and shape parameters were calculated from the contoured ROIs using Eqs. (2) and (3). The performance of the parameters in discriminating normal neck tissue from fibrotic irradiated tissue was evaluated using the probability value (*i.e.*, p value) calculated from the unpaired t -test.

Results

Subjects

Forty subjects were enrolled and classified into three subgroups: (1) the control group consisted of 12 healthy volunteers (6 males and 6 females; mean age: 52.0 ± 11.0 years); (2) the asymptomatic group consisted of 11 post-RT patients who had experience Grade 0 neck fibrosis based on self assessment at follow-up (mean 21.8 ± 7.8 months); (3) the symptomatic group of 17 patients who experienced grade 1 to 3 neck fibrosis at follow-up (mean 17.9 ± 8.9 months).

Patient information and treatment characteristics are presented in Table 1. All post-RT patients received intensity modulated radiation therapy (IMRT) for treatment of head-and-neck malignancy. Three left sides of the asymptomatic group, and one right and one left sides in the symptomatic group were excluded based on the homogeneity criteria. In the symptomatic group, six patients had unilateral neck dissections and two had bilateral neck dissections. In the asymptomatic group, three patients had unilateral neck dissections. All symptomatic patients received chemotherapy: 9 received concurrent cisplatin, 3 received concurrent carboplatin, 1 received induction docetaxel, cisplatin, and 5-fluorouracil (TPF) followed by concurrent cisplatin, and 1 received induction TPF followed by concurrent cetuximab, 1 received concurrent cisplatin and cetuximab, 1 received concurrent cetuximab, and 1 received one cycle of concurrent cisplatin and switched to concurrent cetuximab. In the asymptomatic group, 8 of 11 patients received chemotherapy: 4 concurrent cisplatin, 2 induction TPF followed by concurrent carboplatin, 1 concurrent TPF, and 1 concurrent carboplatin.

Clinical evaluations of neck fibrosis

Physician-based assessments of bilateral neck fibrosis were performed: 2 patients missed physician's assessments, 13 (46.4%) patients were rated grade 0, 7 (25%) were rate grade 1, 4 (14.2%) were rated grade 2, and 1 (3.6%) was rated grade 3 fibrosis. In addition, one patient was graded 1 on the right neck and 2 on the left neck. Patient-based assessments of bilateral neck fibrosis were performed: 16 patients self rated grade 0, 9 self rated grade 1, 1 self rated grade 2, and 1 self rated grade 3 fibrosis. In addition, one patient rated grade 0 for the right neck and grade 1 for the left neck.

Comparing physician-based evaluation with patient-based assessment, ratings of neck fibrosis on 16 (57.1%) patients were the same. Ratings on 12 patients had discrepancies: 5 patients self rated grade 0 fibrosis while physician rated grade 1 on 4 of them and grade2 on 1 patient; 2 patients self rated grade 1 fibrosis while physician rated grade 0; 3 patients rated fibrosis level lower than physician; and 1 patient rated higher than the physician.

Ultrasound Nakagami Imaging of fibrosis-Representative Cases

The Nakagami PDF, shape and scaling parameters of the neck images were generated according to the algorithmic procedure described above. A color map was created to emphasize the contrast in Nakagami parameter values from the smallest (blue) to largest values (red). It should be noted the Nakagami parameters images shown in color are distinct

from Doppler images, which display tissue vasculature. Three representative cases were selected, one from each group, for presentation (Figure 2 shows the results from the right neck).

Normal case (Fig. 1, column 1): B-mode ultrasound image of the left neck of a 43-year-old female healthy volunteer shows the skin and subcutaneous tissue. From the Nakagami imaging, the mean Nakagami PDF value of the right neck was $(8.34 \pm 0.92) \times 10^{-5}$; the mean Nakagami shape value was 0.79 ± 0.07 ; and the mean Nakagami scaling parameter value was $(0.93 \pm 0.22) \times 10^8$.

Asymptomatic case (Fig. 1, column 2): A 62-year-old male had received IMRT for squamous cell carcinoma of the posterior oropharynx. The primary tumor received a total dose of 70.29 Gy and the right neck received 57.75 Gy. The patient was treated from September to November 2009 and ultrasound scanning occurred 17 months after treatment completion. Physician's clinical assessment revealed Grade 1 late toxicity; however the patient rated grade 0 (no symptoms) at the time of follow-up. For the irradiated asymptomatic right neck, the mean Nakagami PDF value was $(4.41 \pm 0.98) \times 10^{-5}$; the mean Nakagami shape value was 1.03 ± 0.18 ; and the mean Nakagami scaling parameter value was $(2.76 \pm 0.37) \times 10^8$.

Symptomatic case I (Fig. 1, column 3): High hyperechoic (brighter) lines or spots due to increased tissue stiffness are visible on the B-mode images of a 60-year-old male post RT who was treated for squamous cell carcinoma of the neck. The primary tumor received a total dose of 70.00 Gy and the right neck region received a mean dose of 60.20 Gy from October to December 2009. At his 13 month follow-up visit, the physician's clinical assessment was Grade 1 fibrosis and the patient experienced Grade 2 (moderate) neck fibrosis. For the post-RT right left region, the mean Nakagami PDF value was $(3.51 \pm 0.47) \times 10^{-5}$; the mean Nakagami shape value was 1.74 ± 0.75 ; and the mean Nakagami scaling parameter value was $(4.26 \pm 0.65) \times 10^8$.

While radiation-induced tissue injury may not be obvious on the ultrasound B-mode images, the radiation-induced changes in the subcutaneous tissues were captured by the Nakagami parameter values. Increases in Nakagami shape and scaling parameter values of the post-RT patients compared to those of the healthy volunteer are evidence on these Nakagami color images. The robustness of the 10 ultrasound Nakagami imaging in quantifying radiation-induced neck fibrosis is further demonstrated in a case of a 62 year female patient. She had received 72 Gy to the primary tumor (squamous cell carcinoma of left ear and external auditory canal). As shown in Figure 2, the light green regions on the neck represented the regions where ultrasound scans were performed. The main dose to her right neck region was 10 Gy (range 7.0–15.0 Gy) while the main dose to her left neck was 60.1 Gy (range 58.0–64.0 Gy). At her 18-month follow-up visit, she rated no fibrosis for her right neck and mild fibrosis on her left neck. Figure 3 shows the ultrasound and Nakagami images of the left and right necks. Compared with the right neck (no fibrosis), the Nakagami PDF parameter value of her left neck (with fibrosis) decreased by 65.8%; the Nakagami shape parameter increased by 70.0%; and the Nakagami scaling parameter increased by 57.3%.

Ultrasound Nakagami Imaging of Radiation-Induced fibrosis - Study cohorts

Nakagami PDF-, shape- and scaling-parameter images were generated for all subjects. Figure 4 shows the mean and standard deviation of the Nakagami parameter values vs. physician-based and patient-based assessments. The Pearson correlation coefficient between physician-based and patient-based fibrosis assessments was 0.38. Statistical analyses confirmed significant differences in all three Nakagami parameters when comparing the control to the post-RT population, and significant differences in Nakagami shape and scaling parameters when comparing the asymptomatic and symptomatic groups. Compared with the control group, the mean Nakagami PDF parameter value decreased by 29.0% for the asymptomatic group and 25.9% for the symptomatic group; the mean Nakagami shape parameter value increased by 32.1% for the asymptomatic group and 74.1% for the symptomatic groups; the average Nakagami scaling parameter value increased by 55.7% for the asymptomatic group and 83.5% for the symptomatic group.

Discussion

In this clinical study, we demonstrated the feasibility of quantifying radiation-induced neck fibrosis. The underlying cellular process of radiation-induced fibrosis is complex involving the up-regulation of mesenchymal cells that over-produce extracellular matrix to replace normal tissue. This change in the tissue's cellular structure produces observable changes in the Nakagami parameters and is the premise behind the ultrasound imaging technique. We have developed ultrasound procedures to measure these changes and define neck fibrosis following head-and-neck RT. Nakagami scaling and shape parameters were estimated from the statistical distribution of the ultrasound RF backscatter and were selected as the most accurate representations of changes in the biomechanical properties of the subcutaneous and underlying tissue. Significant increases in Nakagami parameters were observed among the control, asymptomatic and symptomatic groups.

Although post-RT fibrosis has been recognized for decades, quantifying the severity of fibrosis presents a challenge. The main limitation of the current clinical assessment of fibrosis is the inherent subjectivity in observation and palpation. For example, studies demonstrated a systematic tendency for surgeons to rate fibrosis as more severe than radiation oncologists (21). Reliability studies of clinical fibrosis assessment have presented reliability coefficients widely ranging from 0.23 to 0.76 (21). As shown in our study, major discrepancies were demonstrated between the physician-based evaluation and the patient-based assessment of radiation-induced neck fibrosis. Furthermore, such assessments do not provide sufficient information to characterize the pathophysiology of tissue changes. To address this challenge, Yound *et al.* developed an ultrasound palpation device to measure tissue stiffness and showed its efficacy in the measurement of neck fibrosis in over 100 patients following nasopharyngeal cancer RT (22–24). Unfortunately, such a device's clinical application is limited by the cost of acquiring a new apparatus whose sole purpose is to measure tissue stiffness.

The main strengths of ultrasound Nakagami technology is that the data is acquired using a widely available ultrasound scanner and this computer-aided diagnostic tool does not require the expertise of a radiologist. In addition, the Nakagami parameters yield consistent

measures that are independent of system factors, such as dynamic range and system gain (25), enabling extraction of the weak scattering information that may be lost in the conventional B-mode image interpretation (25). Such subtle changes may be critical in capturing and predicting radiation-induced tissue changes. Future studies will be directed at testing the reliability and reproducibility of our methodology as well as a prospective investigation correlating fibrosis development with clinical signs/symptoms.

Classification of fibrosis severity is a requisite as we attempt to understand the clinical course of fibrosis and develop appropriate treatment strategies. Since toxicity patterns change with new radiotherapy treatment regimens and with adjuvant surgery or chemotherapy, methods to define and monitor new radiation-related toxicities are important goals for all cancer subspecialties. While this report has addressed fibrosis from head-and-neck radiotherapy, the underlying principles and analyses are applicable to treatment of other malignancy sites, such as the breast and soft-tissue. Accurate measurement of radiation-induced fibrosis becomes crucial as radiation oncologists investigate new techniques that reduce treatment morbidity through variations in fractionation schedule, radiation dosage, delivery method, and chemotherapy regimen.

Conclusions

Ultrasound Nakagami imaging, which complements conventional B-mode imaging, has the potential of providing key imaging signatures for the characterization and quantification of radiation-induced neck fibrosis. Ultrasound Nakagami parameters are able to provide statistical features of soft tissues by removing measurement artifacts and providing objective, quantitative, statistical descriptions of tissue microstructures. This preliminary study demonstrated the clinical feasibility and significant differences in Nakagami shape and scaling parameters of the neck tissue between asymptomatic and symptomatic patients within the post-RT groups. Nakagami methods may provide a useful metric of fibrosis secondary to radiation that can be further developed into a low-cost tool for normal-tissue assessment following head-and-neck radiotherapy.

Acknowledgments

Funding information: DOD W81XWH-13-1-0269 and NCI CA114313

References

1. Bentzen SM, Overgaard M. Clinical Radiobiology and Normal-Tissue Morbidity after Breast-Cancer-Treatment. *Advances in Radiation Biology*. 1994; 18:25–51.
2. Bentzen SM, Thames HD, Overgaard M. Latent-Time Estimation for Late Cutaneous and Subcutaneous Radiation Reactions in a Single-Follow-up Clinical-Study. *Radiotherapy and Oncology*. 1989; 15:267–274. [PubMed: 2772254]
3. Dische S, Saunders M, Barrett A, et al. A randomised multicentre trial of CHART versus conventional radiotherapy in head and neck cancer. *Radiotherapy and Oncology*. 1997; 44:123–136. [PubMed: 9288840]
4. Small, W.; Woloschak, GE. *Radiation Toxicity: A Practical Guide*. Vol. 128. Springer US; 2006.
5. Bentzen SM, Dische S. Morbidity related to axillary irradiation in the treatment of breast cancer. *Acta Oncologica*. 2000; 39:337–347. [PubMed: 10987231]

6. Bentzen SM, Overgaard M, Thames HD. Fractionation Sensitivity of a Functional Endpoint - Impaired Shoulder Movement after Post-Mastectomy Radiotherapy. *International Journal of Radiation Oncology Biology Physics*. 1989; 17:531–537.
7. Hojris I, Andersen J, Overgaard M, et al. Late treatment-related morbidity in breast cancer patients randomized to postmastectomy radiotherapy and systemic treatment versus systemic treatment alone. *Acta Oncologica*. 2000; 39:355–372. [PubMed: 10987233]
8. Johansson S, Svensson H, Denekamp J. Dose response and latency for radiation-induced fibrosis, edema, and neuropathy in breast cancer patients. *International Journal of Radiation Oncology Biology Physics*. 2002; 52:1207–1219.
9. Jeraj R, Cao Y, Ten Haken RK, et al. Imaging for Assessment of Radiation-Induced Normal Tissue Effects. *International Journal of Radiation Oncology Biology Physics*. 2010; 76:S140–S144.
10. Delanian S, Lefaix JL. Current management for late normal tissue injury: Radiation-induced fibrosis and necrosis. *Seminars in Radiation Oncology*. 2007; 17:99–107. [PubMed: 17395040]
11. Bentzen SM. Preventing or reducing late side effects of radiation therapy: radiobiology meets molecular pathology. *Nature Reviews Cancer*. 2006; 6:702–713.
12. Liao YY, Tsui PH, Yeh CK. Classification of Benign and Malignant Breast Tumors by Ultrasound B-scan and Nakagami-based Images. *Journal of Medical and Biological Engineering*. 2010; 30:307–312.
13. Liao YY, Li CH, Tsui PH, et al. Strain-compounding technique with ultrasound Nakagami imaging for distinguishing between benign and malignant breast tumors. *Medical Physics*. 2012; 39:2325–2333. [PubMed: 22559602]
14. Ho MC, Lin JJ, Shu YC, et al. Using ultrasound Nakagami imaging to assess liver fibrosis in rats. *Ultrasonics*. 2012; 52:215–222. [PubMed: 21907377]
15. Cox JD, Stetz J, Pajak TF. Toxicity Criteria of the Radiation-Therapy Oncology Group (Rtog) and the European-Organization-for-Research-and-Treatment-of-Cancer (Eortc). *International Journal of Radiation Oncology Biology Physics*. 1995; 31:1341–1346.
16. Shankar PM. Ultrasonic tissue characterization using a generalized Nakagami model. *Ieee Transactions on Ultrasonics Ferroelectrics and Frequency Control*. 2001; 48:1716–1720.
17. Tsui PH, Yeh CK, Liao YY, et al. Ultrasonic Nakagami imaging: a strategy to visualize the scatterer properties of benign and malignant breast tumors. *Ultrasound Med Biol*. 2010; 36:209–217. [PubMed: 20018436]
18. Wagner RF, Insana MF, Brown DG. Statistical properties of radio-frequency and envelope-detected signals with applications to medical ultrasound. *J Opt Soc Am A*. 1987; 4:910–922. [PubMed: 3298583]
19. XXX
20. XXX
21. Davis AM, Dische S, Gerber L, et al. Measuring postirradiation subcutaneous soft-tissue fibrosis: State-of-the-art and future directions. *Seminars in Radiation Oncology*. 2003; 13:203–213. [PubMed: 12903010]
22. Zheng YP, Leung SF, Mak AFT. Assessment of neck tissue fibrosis using an ultrasound palpation system: a feasibility study. *Medical & Biological Engineering & Computing*. 2000; 38:497–502. [PubMed: 11094804]
23. Balbir-Gurman A, Denton CP, Nichols B, et al. Non-invasive measurement of biomechanical skin properties in systemic sclerosis. *Ann Rheum Dis*. 2002; 61:237–241. [PubMed: 11830429]
24. Leung SF, Zheng Y, Choi CY, et al. Quantitative measurement of post-irradiation neck fibrosis based on the young modulus: description of a new method and clinical results. *Cancer*. 2002; 95:656–662. [PubMed: 12209759]
25. Tsui PH, Chang CC. Imaging local scatterer concentrations by the Nakagami statistical model. *Ultrasound in Medicine and Biology*. 2007; 33:608–619. [PubMed: 17343979]

Summary

Fibrosis is a common long-term complication of cancer radiotherapy. Standard clinical assessment of subcutaneous fibrosis is subjective and often limited to visual inspection and palpation. Ultrasound Nakagami imaging is investigated as a safe, objective and easy-to-use imaging technique to assess the severity of neck fibrosis following head-and-neck radiotherapy. Nakagami parameters may provide a useful metric of fibrosis secondary to radiation that can be further developed into a low-cost tool for normal-tissue assessment following head-and-neck radiotherapy.

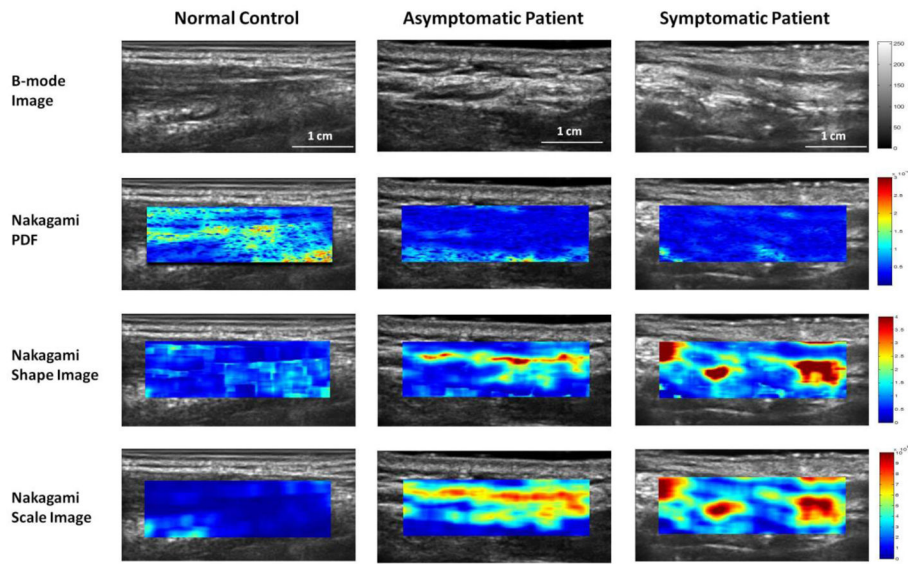


Figure 1. B-mode and Nakagami parameter images of the right neck of a healthy volunteer (column 1), asymptomatic (column 2) and symptomatic patient (column 3). Row 1: B-mode image; Row 2: Nakagami-PDF image; Row 3: Nakagami-shape image; and Row 4: Nakagami-scaling image. Compared with the normal neck, smaller Nakagami PDF, and greater Nakagami shape and scaling parameter values were observed in the post-RT patients.

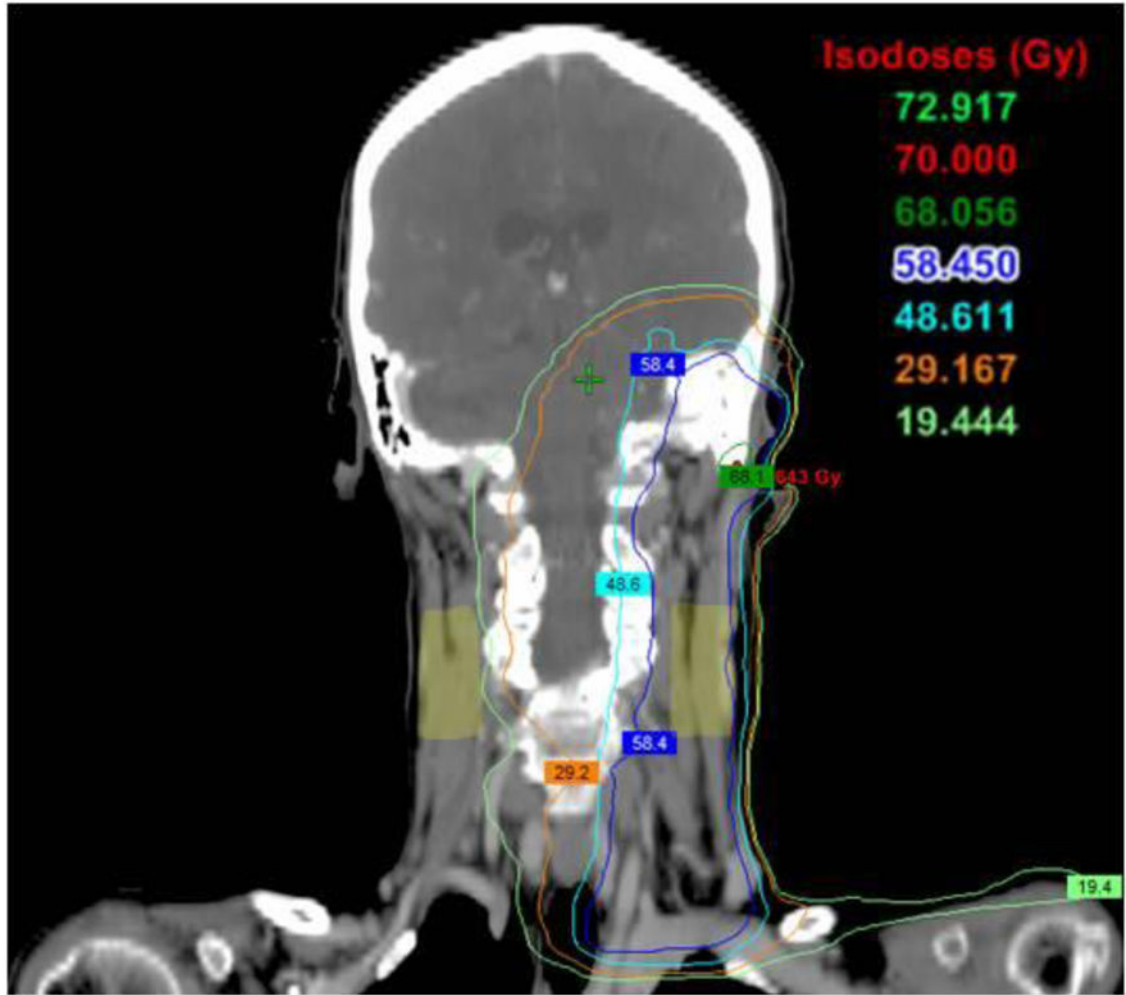


Figure 2. Dose distribution of the neck regions of a 62-year old woman received IMRT for head-and-neck cancer. Ultrasound scans were performed on the bilateral neck (light green regions). The mean dose was 10 Gy in the right and 60.1 Gy to the left neck regions.

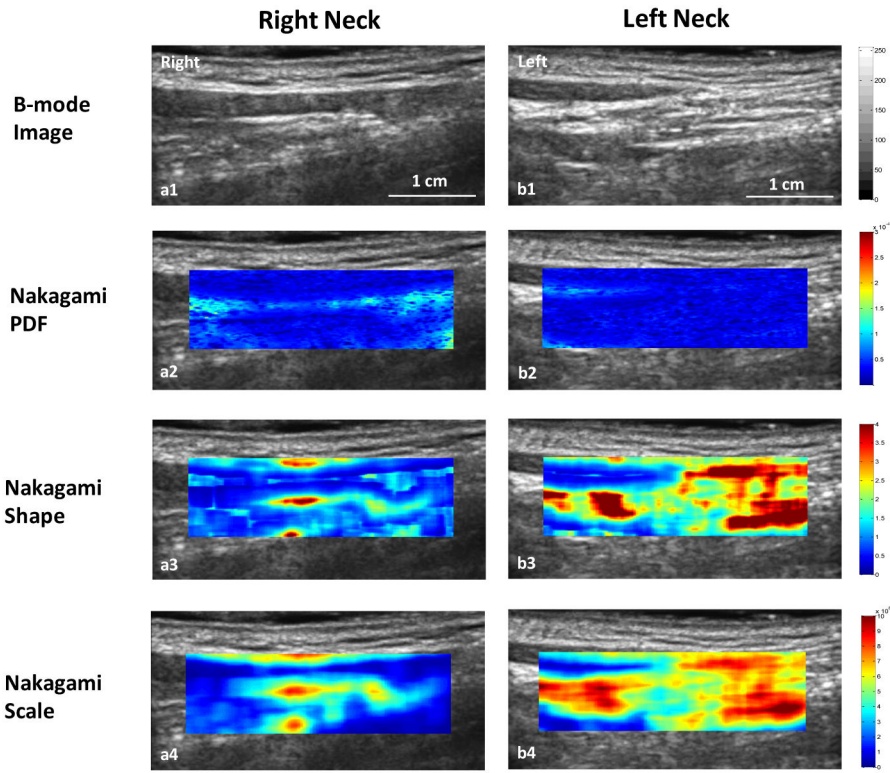


Figure 3. Nakagami imaging comparison of the right neck (right column) and left neck (left column) and. Row 1: B-mode image; Row 2: Nakagami-PDF image; Row 3: Nakagami shape image; and Row 4: Nakagami-scaling image. Compared with the right neck, lower Nakagami PDF and higher Nakagami shape and scaling parameter values were observed in the left neck area with fibrosis.

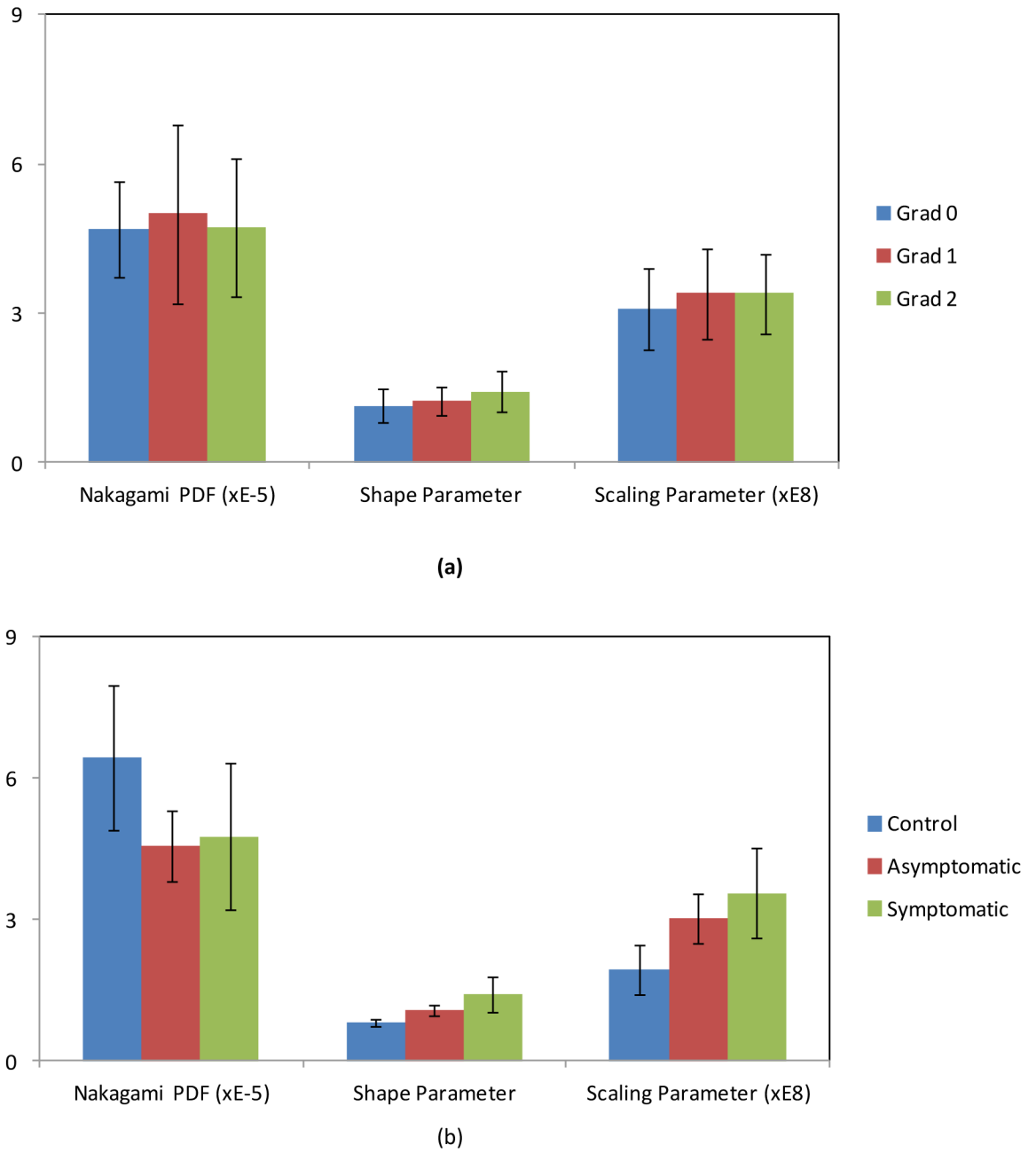


Figure 4. The mean and standard deviation of the Nakagami parameter values vs. physician-based (a) and patientbased assessments (b).

Table 1

Patient and treatment characteristics

Characteristics		Post-RT Asymptomatic Group	Post-RT Symptomatic Group	
Age (years)		61.1 ± 9.6	56.8 ± 7.8	
Gender	Male	9	12	
	Female	2	5	
Primary tumor site	Oropharynx/Nasopharynx	1	2	
	Larynx	1	3	
	Oral cavity	4	9	
	Tonsil	3	2	
	Salivary gland	2	1	
Histology	Squamous cell carcinoma	8	17	
	Adenocarcinoma	2	0	
	Mucoepidermoid carcinoma	1	0	
TNM stage	T stage	T1	1	3
		T2	4	2
		T3	1	2
		T4	5	7
		Tx	0	3
	N stage	N0	4	3
		N1	0	1
		N2	6	8
		N3	1	4
		Nx	0	1
M stage	MX	3	0	
	M0	8	17	
Mean dose to the neck (Gy)	Right	59.8 ± 3.0	61.1 ± 2.5	
	Left	59.3 ± 3.1	59.2 ± 2.9	
Follow-up time (months)		21.8 ± 7.9	19.7 ± 8.9	

Table 2

(a) Nakagami parameters vs. physician-based assessments of neck fibrosis			
Groups	Nakagami PDF (10^{-5})	Shape parameter	Scaling parameter (10^8)
Post-RT Grad 0 Group (n=13)	4.70 ± 0.96	1.14 ± 0.33	3.09 ± 0.82
Post-RT Grad 1 Group (n=7)	5.00 ± 1.80	1.24 ± 0.27	3.39 ± 0.91
Post-RT Grad 2 Group (n=6)	4.71 ± 1.39	1.43 ± 0.40	3.40 ± 0.80
<i>P-value (Grad 0 vs. Grad 1 Post-RT)</i>	0.271	0.146	0.149
<i>P-value (Grad 0 vs. Grad 2 Post-RT)</i>	0.482	0.017	0.136
<i>P-value (Grad 1 vs. Grad 2 Post-RT)</i>	0.315	0.081	0.493

(b) Nakagami parameters vs. patient-based assessments of neck fibrosis			
Groups	Nakagami PDF (10^{-5})	Shape parameter	Scaling parameter (10^8)
Control Group (n=12)	6.44 ± 1.55	0.81 ± 0.08	1.94 ± 0.51
Post-RT Asymptomatic Group (n=11)	4.57 ± 0.76	1.07 ± 0.11	3.02 ± 0.52
Post-RT Symptomatic Group (n=12)	4.77 ± 1.57	1.41 ± 0.39	3.56 ± 0.95
<i>P-value (Control vs. Asymptomatic Post-RT)</i>	<0.001	<0.001	<0.001
<i>P-value (Control vs. Symptomatic Post-RT)</i>	<0.001	<0.001	<0.001
<i>P-value (Symptomatic Post-RT vs. Asymptomatic Post-RT)</i>	0.271	<0.001	0.005
<i>P-value (Control vs. Post-RT)</i>	<0.001	<0.001	<0.001